Chapter 4
Meridional Heat Convergence Will Increase Tropical North Atlantic Heat Content Available for Hurricane Intensification

Elizabeth Harris, Dipanjan Dey, Robert Marsh, and Jeremy Grist

Abstract Ocean heat content available for hurricane intensification is expected to increase in a warming world. Mechanisms for growth of the Atlantic Warm Pool to 2050 are examined in a high-resolution coupled ocean and atmosphere model with greenhouse gas forcing. The model warm pool increases in depth as well as northern and eastern extent. While net heat flux from the atmosphere remains stable through the forced model run, heat convergence from reduced heat transport by ocean currents drives growth of the warm pool. While atmospheric heat flux and oceanic heat convergence both contribute to anomalous warm water for hurricane development at present, high resolution ocean modelling suggests that, when atmospheric conditions allow for hurricane formation, increased potential for intensification from a warmer ocean will primarily be due to reduced meridional heat transport.

Keywords Climate change · Heat content · Hurricanes · Meridional transport · Warm pool · Heat convergence

Key Points:
- The volume of warm water increases to the north, east, and in depth, in a high-resolution ocean model with high emissions forcing.

E. Harris (✉)
School of Ocean and Earth Science, University of Southampton, Southampton, UK

Ariel Re, Bermuda, Hamilton, Bermuda
e-mail: elizabeth.harris@arielre.com

D. Dey
School of Ocean and Earth Science, University of Southampton, Southampton, UK

School of Earth, Ocean and Climate Sciences, Indian Institute of Technology, Bhubaneswar, India

R. Marsh
School of Ocean and Earth Science, University of Southampton, Southampton, UK

J. Grist
National Oceanography Centre, Southampton, UK

J. Collins et al. (eds.), *Advances in Hurricane Risk in a Changing Climate*, Hurricane Risk 3, https://doi.org/10.1007/978-3-031-63186-3_4

- Convergence of ocean heat transport between 10 °N and 30 °N drives this increase.
- This additional ocean heat content could be available for potential hurricane intensification if atmospheric conditions allow.

4.1 Introduction

Recent US landfalling hurricanes have resulted in more than 40 billion USD in damage (NCEI 2023) in 5 of the last 7 years (2017–2023), bringing to the forefront the need to understand how anthropogenic warming may have contributed to the intensity of these events, and how major hurricanes could develop in a future, warmer climate.

An increasing area of warm tropical Atlantic sea surface temperature (SST) since the 1970s has provided a larger energy source for hurricane intensification (Saunders and Lea 2008). The Atlantic Warm Pool (AWP) has maintained feedback loops resulting in lower wind shear and a moist atmosphere (Wang and Lee 2007). Annual Atlantic basin major hurricane counts exhibit an increasing trend in the last few decades (Vecchi et al. 2021), mainly due to a recovery from anomalously low activity in the 1970s and 80s, compared with subsequent decades (Nyberg et al. 2007; Rousseau-Rizzi and Emanuel 2022). Recent high major hurricane landfall activity since 2017 (Murakami et al. 2018) marked a return to expected behaviour due to warming Atlantic SSTs, after an unusual gap in the record (Hall and Hereid 2015). When changes in the observational network are accounted for, there remains significant multidecadal variability, but little upward trend since the 1850s (Vecchi et al. 2021). There is also no upward long-term trend in US landfalling major hurricanes since 1900 (Klotzbach et al. 2018), a record which offers reasonable consistency since the onset of anthropogenic warming, as few of these storms are likely to have been missed.

Observed multi-decadal variability in Atlantic major hurricane activity has been explained by a cool period in the North Atlantic resulting from a combination of sulphate aerosol emissions (Dunstone et al. 2013) and natural variability in ocean circulation (Yan et al. 2017; Zhang et al. 2019). It is difficult to separate the potential impact of climate change on major hurricane frequency from these other atmospheric and oceanic factors which have influenced activity on multidecadal timescales; for example, while Kang and Elsner (2015) found a recent increase in global tropical cyclone (TC) intensity, they do not attribute it to climate change. More generally, while a recent review (Knutson et al. 2019) found mixed evidence to support conjectures that an increase in major hurricane activity has already occurred, continued warming of the tropical ocean due to greenhouse gas forcing could provide the potential for additional hurricane intensification in future decades, provided atmospheric conditions permit tropical cyclone development.

Climate models systematically underestimate the number and strength of tropical cyclones (Walsh et al. 2016). Tropical cyclone activity is simulated in

high-resolution climate modelling, HADGEM3-GC31-HH, but projected changes for the North Atlantic are inconclusive, particularly as major hurricanes are not produced by even the highest resolution climate models (Roberts et al. 2020a; Davis 2018). A number of future model projections using downscaling techniques predict a lower frequency of global tropical cyclones, and an increase in the proportion of the most intense storms (Knutson et al. 2020). In general, the reliability of future projections is challenged by the low annual frequency and large variability of TCs (Yoshida et al. 2017). While truly understanding the mechanisms of TC frequency and resolving extreme TCs accurately within climate models remains elusive (Sobel et al. 2021), they can provide insight into the processes which will drive future TC changes.

For example, the Atlantic Meridional Overturning Circulation (AMOC) is predicted to decrease in strength due to increased freshwater at high latitudes reducing deep water formation (Madan et al. 2023), as polar ice caps melt. This allows accumulation of heat in the tropical Atlantic. Variation in inter-model AMOC strength remains a major factor in future climate uncertainty (Bellomo et al. 2021). Liu et al. (2013) consider the historical runs of 19 CMIP5 models, many of which exhibit a cold SST bias in the tropical Atlantic. While this cold bias still exists in CMIP6, higher resolution models more realistically represent ocean processes, so the impacts of continued greenhouse gas warming can be anticipated with greater confidence. Han et al. (2021) examined 33 CMIP6 models and found that model reanalysis skill for tropical cyclone predictor climatology and interannual variability improves with higher horizontal resolution, including tropical SST. This is likely due to the better representation of northwards heat transport via the AMOC (Roberts et al. 2020b), due to increased ocean resolution, as well as improvements in parameterization of the surface mixed layer and interior mixing processes.

Climate models provide projections of the atmospheric variables relevant to hurricane activity, including atmospheric stability, humidity, and vertical wind shear (VWS) (DeMaria et al. 2001). Tang and Camargo (2014) propose an index for tropical cyclone activity including VWS, entropy, and potential intensity, from analysis of CMIP5 models. Tropical Atlantic VWS, the strength of which is associated with the El Niño Southern Oscillation (ENSO) on interannual timescales, is stronger in climate model projections (Vecchi and Soden 2007; Emanuel 2021), inhibiting hurricane development (Lin et al. 2020). Atlantic VWS exhibits Interseasonal and intraseasonal variability (Aiyyer and Thorncroft 2006), leaving windows of opportunity for hurricane development, given existing disturbances and warm SSTs.

Historically, a warmer tropical Atlantic has been linked with increased hurricane activity (Goldenberg et al. 2001; Moharana and Swain 2023). Warm water is primarily defined here as warmer than 26.5 °C. This has been identified as the threshold temperature for most hurricane development in previous studies (Dare and McBride 2011; McTaggart-Cowan et al. 2015). Johnson and Xie (2010) note covariability in tropical SST and convection in satellite precipitation, while Dare and McBride (2011) find that the temperature threshold directly related to tropical cyclogenesis has not been observed to have changed significantly during

1981–2008. However, based on climate model analyses, it has been proposed that the temperature threshold for tropical deep convection could vary with the climate state (Evans and Waters 2012; Korty et al. 2012; Sugi et al. 2015). Nevertheless, many studies confirm the importance of ocean heat content as a critical ingredient of increased tropical cyclone activity and in model TC simulation (Chan et al. 2021; Hallam et al. 2021; Domingues et al. 2019; Pfleiderer et al. 2022). The goal here is not to resolve this issue but to diagnose the source of increased ocean heat which will be available for potential TC development when atmospheric conditions allow.

In general, there is low confidence in observed long-term change in major hurricane frequency and uncertainty in their future projections. However, further growth in the amount of warm water available to fuel intense hurricanes would be one factor which could impact Atlantic basin activity in the next few decades. Climate models using high-resolution ocean models can improve projections of hurricane climate predictors, particularly the region of warm water available for hurricane development. In this study, the potential future change in the volume of warm water available for hurricane development is quantified using the HadGEM3-GC31-HH high-resolution climate model with prescribed greenhouse gas forcing following the Shared Socioeconomic Pathway 585 (SSP585) high emissions scenario.

In summary, although climate models suggest that variables other than SST may drive future tropical cyclone frequency, increasing ocean heat content is widely understood to explain recent increases in hurricane activity. Hence the drivers of warm water volume variability in an increasingly warm, forced climate are examined here, including air-sea heat flux into the ocean, and advective heat convergence across the tropical Atlantic. The robustness of the advective heat convergence trend is tested by extending the analysis to three other high-resolution climate models.

4.2 Data and Methods

4.2.1 CMIP6 HighResMIP (High-Resolution Model Intercomparison Project)

High-resolution coupled climate model output is analysed from experiments described by Haarsma et al. (2016). These models start with a short spin-up period of 30 to 50 years and then are run from 1950 through 2050. The control run external forcing is at 1950 levels. Historical forcing is used in years 1950 to 2014. The SSP585 high emissions scenario forcing, where radiative forcing increases to 8.5 Wm^{-2} by 2100, is applied during 2015 to 2050.

Our primary focus in this study is analysing the outputs from the high-resolution ocean and atmosphere model HadGEM3-GC31-HH (Roberts et al. 2019), which includes the project's (HighResMIP) highest resolution ocean configuration, at 1/12°. The ocean model is the Nucleus for European Modelling of the Ocean

Table 4.1 HighResMIP Model configurations

			Horizontal resolution	
Model	Resolution name	Ocean model	Ocean	Atmosphere (km)
HadGEM3-GC31	HH	NEMO 3.6	1/12°	50
HadGEM3-GC31	HM	NEMO 3.6	1/4°	50
EC-Earth3P	HR	NEMO 3.6	1/4°	50
CESM1-3	HH	POP	1/10°	25

(NEMO) version 3.6 (Madec et al. 2017), with 75 levels. Atmospheric resolution is 50 km.

To sample the diversity of model configuration and resolution, we compare data from three other high-resolution models (Table 4.1), including HadGEM3-GC31-HM with a lower resolution ocean model, at 1/4° (HM), EC-Earth3P (ECE), with a similar configuration to HM (Haarsma et al. 2020), and CESM1-3 (CESM), which uses the POP ocean model at 1/10° horizontal resolution (Danabasoglu et al. 2012; Small et al. 2014), with 25 km atmospheric resolution.

4.2.2 Ocean Data

The observed volume of Atlantic water warmer than specific temperature thresholds, north of 10 °N, was calculated using the UK Met Office Hadley Centre EN4 subsurface ocean temperature analysis, which provides ocean analysis data from 1900 to the present (Good et al. 2013). This dataset contains gridded subsurface temperature at 42 discrete depths, at 1° latitude longitude horizontal resolution, from 1900 to the present, from 83 °S to 90 °N. While this dataset offers a longer record than other datasets, direct observations used are increasingly scarce with depth and further back in time.

The mean decadal observed depth of the 26.5 °C isotherm, north of 10 °N, was calculated using the National Center for Environmental Prediction (NCEP) Global Ocean Data Assimilation System (GODAS) ocean reanalysis product (Behringer and Xue 2004). This dataset contains gridded global potential temperature at 40 discrete depths, at 1/3° latitude and 1° longitude spacing, from 1980.

4.2.3 Atmospheric and Surface Flux Data

ERA5 (Hersbach et al. 2020) is produced by the Copernicus Climate Change Service (C3S) at the European Centre for Medium-Range Weather Forecasts (ECMWF). It is the fifth generation ECMWF atmospheric reanalysis of the global climate covering the period from January 1940 to the present. Hourly 30 km grid data is aggregated to

monthly averages. Surface latent heat flux, net solar and longwave radiation, and sensible heat flux are used in this analysis.

4.2.4 Hurricane Data

Annual North Atlantic basin major hurricane counts are collected from the International Best Track Archive for Climate Stewardship (IBTrACS) (Knapp et al. 2010; Knapp et al. 2018) Version 4 dataset for the Atlantic basin. This data consists of storm-centred point data from 1851, which includes maximum 1 min mean winds at 6-hourly intervals over the ocean, more frequent near land, rounded to the nearest 5 knots. Unique storms reaching greater than 96 knots of maximum wind speed in their lifetime during 1980 to 2022 are identified here, as recorded by the National Hurricane Center (NHC).

4.2.5 Water Mass Transformation

From the original formulation of Walin (1982), the Water Mass Transformation (WMT) framework (Groeskamp et al. 2019) is applied in temperature space, quantifying volume fluxes across isotherms associated with variations of heat fluxes in that property space. With this diagnostic, we attribute variations in warm water volume to variations in surface heat exchanges. The net surface heat flux, Q_{net}, combines surface net solar radiation (Q_{sw}), net longwave radiation (Q_{lw}), sensible heat flux (Q_{sh}), and latent heat flux (Q_{lh}). Throughout this study, the convention is that all heat fluxes are positive into the ocean:

$$Q_{net} = Q_{sw} + Q_{lw} + Q_{sh} + Q_{lh} \tag{4.1}$$

Across temperature space, the volume of water transformed by Q_{net} is calculated over the North Atlantic, north of 10 °N, where tropical storms are able to form due to sufficient Coriolis acceleration. Firstly, the Diathermal Temperature Flux, $Q_{in}(T)$ (°C m^3 s^{-1}) (2), is found by area-integrating Q_{net}, where SST is at or above a given value of temperature, T, then dividing by reference density, ρ_0, and specific heat capacity, c_p:

$$Q_{in}(T) = \frac{1}{\rho_o c_p} \int_{x_w}^{x_e} \int_{y_s}^{y_n} Q_{net}(x,y)\Gamma(SST(x,y),T)dxdy \tag{4.2}$$

where x, y are distance in west (w) to east (e) and south (s) to north (n) directions, and Γ is a sampling function; Γ = 1 where SST > T, otherwise Γ = 0. Q_{net} values at the potential temperature grid points are found using bilinear interpolation.

The thermal water mass transformation rate, $F_T(T)$ ($m^3 s^{-1}$), can then be arrived at by taking differences between $Q_{in}(T)$ across two temperature surfaces:

$$F_T(T - \Delta T/2, T + \Delta T/2) = \frac{Q_{in}(T - \Delta T/2) - Q_{in}(T + \Delta T/2)}{\Delta T} \tag{4.3}$$

The WMT framework is used here to diagnose the contribution of heat flux trends from air-sea interaction to the evolving volume of warm water in the tropical North Atlantic in a warming future climate.

4.2.6 Back-Tracking Warm Water (TRACMASS)

The TRACMASS Lagrangian trajectory code has been designed for use with gridded weather and climate models to track water paths and associated heat and salt fluxes (Aldama-Campino et al. 2020; Döös et al. 2017). One of the unique characteristics of TRACMASS is that it uses differential equations and mass transport fields at the grid cell walls to analytically calculate the trajectory path through grid boxes. The use of mass transport in a grid cell makes TRACMASS a mass-conserving algorithm. From changes in temperature along each path, we obtain Lagrangian heat divergences, which are ensemble-averaged to obtain heat input to the northward flow across tropical latitudes. Here we track water paths backwards from latitudes currently relevant to hurricane development for water warmer than 26.5 °C. Water parcels are seeded so there is at least one water path start point per HadGEM3-GC31-HH grid cell.

4.3 Results

4.3.1 Future Trends in Available Heat Content

In this section, we investigate HadGEM3-GC31-HH 1950–2050 predicted changes in the amount of heat potentially available for hurricane intensification. We first evaluate changes in the AWP at various temperature thresholds at the peak of hurricane season in the high-resolution model, referencing observational data for model validation. Timeseries of total volume and area of warm water are presented. Maps of the decadal mean depth of the 26.5 °C isotherm are included to highlight the regional extent of warm water through the forced model run.

The total model volume of water in the North Atlantic north of 10 °N and warmer than 26.5 °C, 27.5 °C and 28.5 °C is summed for the month of September, and plotted over time, in Fig. 4.1. September is the peak of the hurricane season; 48% of major hurricanes intensified to 96 knots or above in this month during 1900–2023. The forced run is compared with the control run and EN4 observations.

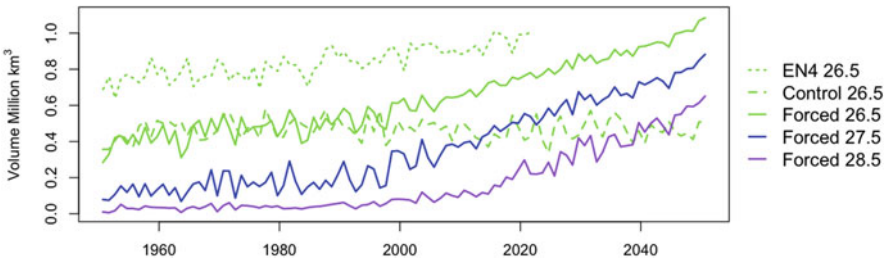

Fig. 4.1 September HadGEM3-GC31-HH 1950–2050 forced run mean monthly volume (million km^3) in the North Atlantic north of 10 °N of water warmer than 26.5 °C (green, solid), 27.5 °C (blue), and 28.5 °C (purple); warmer than 26.5 °C in the control run (green, dashed), and EN4 1950–2022 (green, dotted)

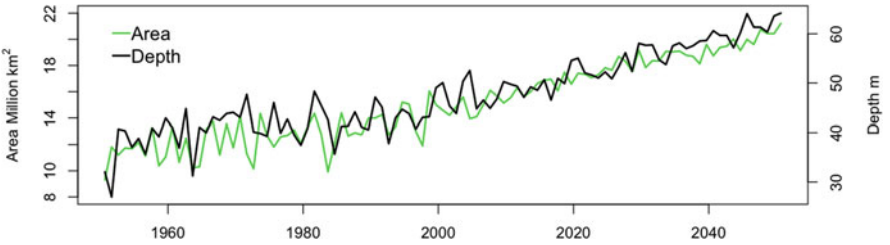

Fig. 4.2 September mean monthly area of water (million km^2) warmer than 26.5 °C in the North Atlantic north of 10 °N: HadGEM3-GC31-HH 1950–2050 forced run (green) and depth of the 26.5 °C isotherm (black)

The HadGEM3-GC31-HH September volume of warm water (> 26.5 °C) increases gradually from 1950 to around 2000, after which it increases rapidly with additional external forcing in the model high emissions forced years. The 1950–1959 September mean monthly volume warmer than 26.5 °C is 0.40 million km^3. In the final decade of the years with historical forcing, 2005–2014, the mean September volume of warm water has reached 0.64 million km^3, an increase of 0.04 million km^3 per decade. The rate of change increases with time in the forced run. The model predicts 0.96 million km^3 by 2040–2049, an increase of 0.08 million km^3 per decade compared with the volume at the end of the period with historical forcing. Hence, the model predicts 56% more warm water by the middle of the twenty-first century, with high emissions forcing. The trend in observed September volume of water warmer than 26.5 °C is an increase of 0.003 million km^3 per year. The model cool bias in the tropical North Atlantic is clear, as the EN4 monthly mean warm water volume (> 26.5 °C) in is nearly twice as large as the warm water volume in the high-resolution model.

HadGEM3-GC31-HH mean monthly area and depth of water warmer than 26.5 °C in the North Atlantic north of 10 °N in September is shown in Fig. 4.2. As with warm water volume, the area at the surface also increases, with an increase in the rate of change in the forced run. The mean depth of the September 26.5 °C

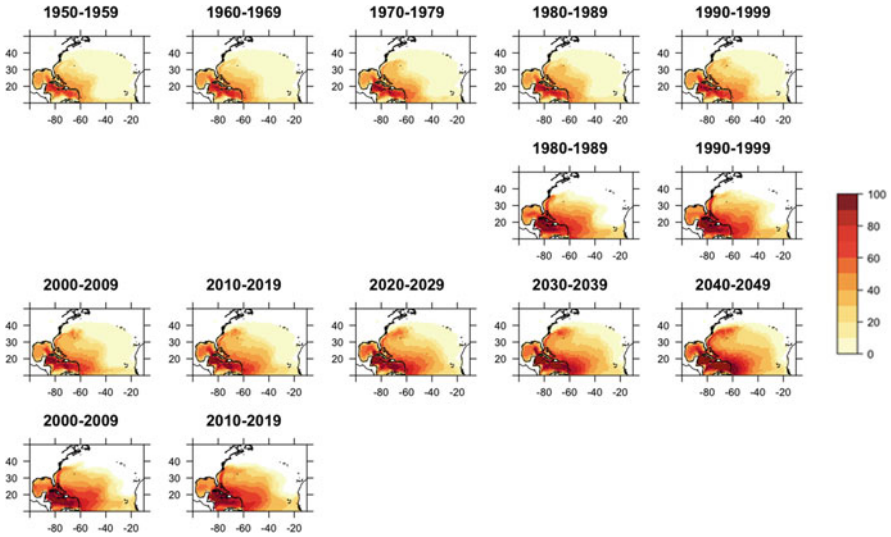

Fig. 4.3 Depth of the September 26.5 °C isotherm (m) in the North Atlantic north of 10 °N by decade 1950–2049 HadGEM3-GC31-HH forced run (rows 1 and 3) and 1980–2019 GODAS (rows 2 and 4)

isotherm north of 10 °N also continues to increase in the high emissions years of the forced run. Both the area and depth of the warm water pool increases, so volume changes are not only the result of both increasing area and depth of the 26.5 °C isotherm with atmospheric forcing.

The depth of the HadGEM3-GC31-HH forced September 26.5 °C isotherm is plotted by decade, providing spatial insight into the depth and extent of the AWP (Fig. 4.3, rows 1 and 3). The warm water area expands to the north and east over time and deepens in the Caribbean Sea and western tropical Atlantic. This is compared with GODAS (rows 2 and 4). A larger area of warm water extending vertically to 100 m is evident in the observational data than in the model, due to the HadGEM3-GC31-HH cold bias. A thin layer of warm water (light yellow) extends further to the north and east in the HasGEM3-GC31-HH maps due to higher resolution of vertical levels near the surface than in the GODAS data. GODAS vertical levels have a 10 m resolution in the top 100 m. The much higher resolution of HH vertical levels near the surface do not average out very shallow warm temperatures in surface layers.

The HadGEM3-GC31-HH model predicts a high emissions scenario future with a much larger volume of deep warm water extending further north and east than the present day. In the following sections, we analyse changes in the mechanisms of heat transfer into the tropical North Atlantic, to diagnose which processes drive the projected increase in warm water in high resolution forced models, with a focus on HadGEM3-GC31-HH.

4.3.2 Changes in Atmospheric Heat Flux

Heat exchange between the atmosphere and ocean is a major driver of interannual variability in the volume of warm water in the tropical North Atlantic, particularly through latent heat flux (Hallam et al. 2019). Similarly, an increasing trend in heat flux into the ocean over surface water which flows through the tropical Atlantic would result in an increase in warm water volume. Additional absorption of heat from the atmosphere could be a result of, for example, higher humidity surface conditions decreasing latent heat flux from the ocean by reducing evaporation, and/or decreased cloudiness, allowing additional short-wave radiation absorption into the ocean.

We inspect the main drivers of heat accumulation in the tropical North Atlantic in HadGEM3-GC31-HH, to explain these changes in the warm water pool. HadGEM3-GC31-HH heat flux in the North Atlantic between 10 °N and 30 °N is examined. This covers the region of 26.5 °C water, where 90% of hurricanes intensify into major hurricanes (Fig. 4.4). We then calculate the volume of water transformed across isotherms, using the WMT framework, to quantify the ocean-atmosphere heat exchange driving AWP volume changes.

Figure 4.5 shows a small upward trend in Q_{net} into the ocean in HadGEM3-GC31-HH over the Atlantic between 10 °N and 30 °N in the forced model run. The mean 2015–2050 Q_{net} is 0.04 Wm^{-2} higher than the 1950–2014 mean. This small change in Q_{net} is a consequence of large but compensating changes in the component fluxes (not shown here) in the model. The small change in Q_{net} then suggests that transfer of additional heat from the atmosphere into the ocean at these latitudes is not the driver of increasing AWP by 2050 in the high-resolution model.

Observed (ERA5) Q_{net} is higher into the ocean and exhibits more variability than the model on multidecadal timescales. ERA5 heat input into the ocean has a negative trend in this period of -0.04 Wm^{-2} per year. Mayer et al. (2023) likewise observe a negative trend for a sample location in the tropical North Atlantic, which they suggest is due to global warming.

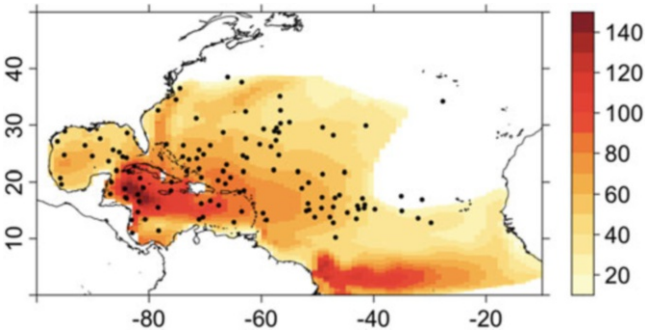

Fig. 4.4 1980–2022 Mean depth of GODAS September 26.5 °C isotherm (m) and IBTrACS points 1980–2022 where hurricanes intensified into major hurricanes

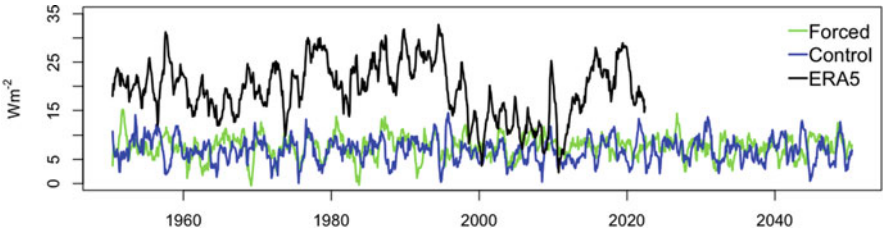

Fig. 4.5 Mean monthly Q_{net} into the Atlantic Ocean (Wm^{-2}) 10 °N to 30 °N with 12-month centred moving average: HadGEM3-GC31-HH 1950–2050 forced run (green) and control (blue), compared with observed ERA5 (black)

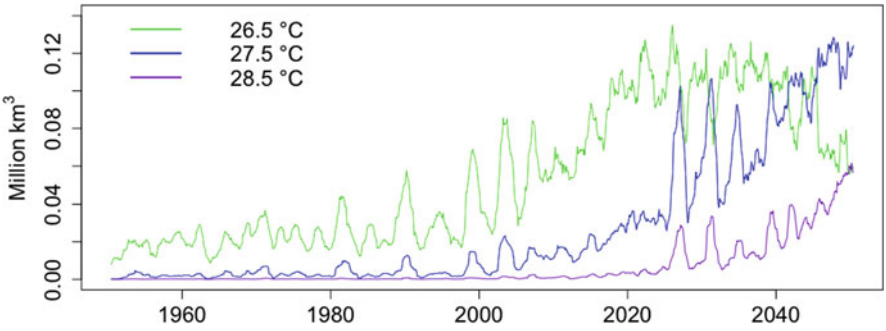

Fig. 4.6 Mean monthly volume (million km^3) of water transformed across the 26.5 °C (green), 27.5 °C (blue) and 28.5 °C (purple) isotherm, with 12-month centred moving average

The volume of water transformed across the isotherms which have historically been relevant to hurricane development in the North Atlantic north of 10 °N can be calculated using the WMT framework (Harris et al. 2022). This metric diagnoses the additional volume of water warmer than these temperature thresholds. The total volume increases due to both deepening of the 26.5 °C isotherm and a larger area of water warmer than 26.5 °C, over which the heat flux into the ocean warms the AWP.

Figure 4.6 indicates the amount of water transformed across the 26.5 °C, 27.5 °C, and 28.5 °C isotherms. For each temperature threshold, the transformed volume is positive from 1950–2050 in the forced run. Using this framework, the rate at which water is transformed by atmospheric heat flux increases around 2000. The transformed volume peaks in the mid-2020s and then begins to decline towards the end of the simulation for water transformed across 26.5 °C, as much of the tropics and subtropics reach this temperature, but continues to increase for higher temperature thresholds.

As the WMT framework calculates the volume transformed by heat flux bounded by the area of water at that temperature, the increase in transformed volume of 26.5 °C water over time must be due to an increasing area of water over which the transformed volume is calculated, rather than an increase in the heat flux into the

ocean, as suggested by the absence of a trend in HadGEM3-GC31-HH atmospheric heat exchange (Fig. 4.5).

The significant increase in the size of the AWP by 2050 in the HadGEM3-GC31-HH forced run cannot be attributable to additional absorption of net heat transfer from the atmosphere as greenhouse gases continue to increase (from Fig. 4.5). Hence, next, we consider the contribution of advective heat flux by ocean currents.

4.3.3 Climate Change and Tropical Atlantic Advective Heat Flux

In this section, the advective component of warm water volume changes in the tropical Atlantic in the HadGEM3-GC31-HH forced run are discussed. Warm water volume convergence between 10 °N and 30 °N is analysed across a suite of 'HighResMIP' ocean models. These models differ by resolution and ocean model, adding robustness to our results. Employing a complementary technique, we also use TRACMASS Lagrangian analysis applied to HadGEM3-GC31-HH forced simulation output to analyse ocean properties and heat convergence along trajectories, and hence, diagnose mechanisms of advective heat transfer into the tropical Atlantic. These trajectories are calculated backwards from 20 °N in the Atlantic for 6 months prior to June 30, near the beginning of the hurricane season.

Figure 4.7 shows the warm water volume convergence between 10 °N and 30 °N. This has been calculated using meridional mass transport from four high-resolution ocean climate models. All models show an increase in warm water convergence between these latitudes at these temperatures. Convergence of water warmer than 26.5 °C increases after 2000 and begins to decrease after 2030. At this time there is still a larger volume of water warmer than 26.5 °C transported across 10 °N than 30 °N. However, the difference between the transport across the higher and lower latitudes decreases, as the AWP extends this far north most of the time by the end of the simulation. At higher temperature thresholds, warm water convergence increases through the model run as the amount of water warmer than these temperatures steadily increases between these latitudes.

HadGEM3-GC31-HM behaves in a similar fashion, although the decline in convergence of 26.5 °C and warmer water is less pronounced than in the HadGEM3-GC31-HH model. The ECE model convergence of 26.5 °C plateaus in the forced run, rather than declines. The CESM model, on the other hand, shows less increase in convergence at any temperature threshold, which may be due to its near-surface warm bias (Roberts et al. 2020b).

Analysis of output of this suite of high-resolution forced ocean models shows an increase in the volume of water warmer in the region of recent hurricane development. The increase in greenhouse gases in the HadGEM3-GC31-HH forced run results in a greater reduction in ocean transport via weakening of the AMOC

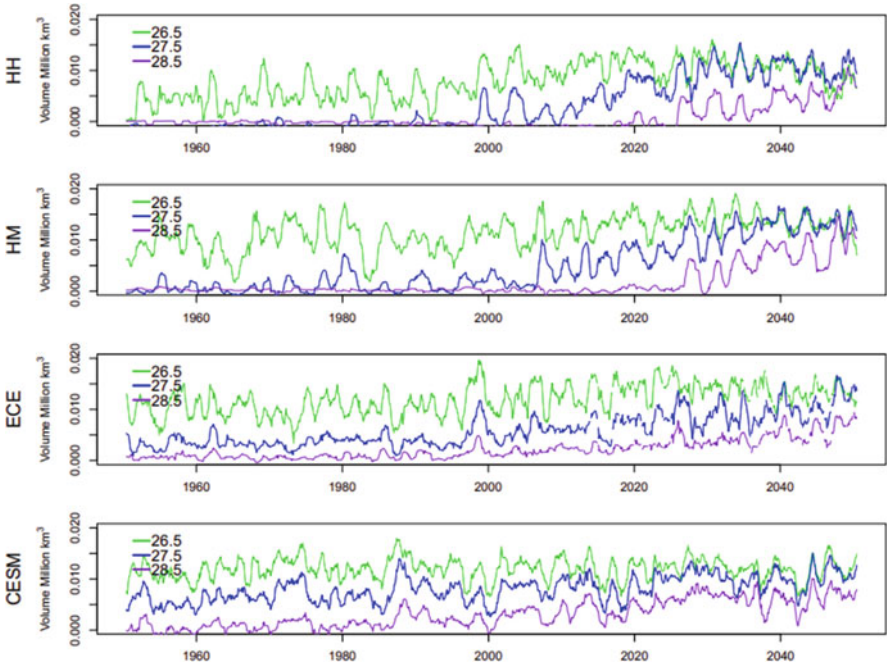

Fig. 4.7 Monthly meridional convergence of warm water volume (million km^3) convergence between 10 °N and 30 °N with 12-month centred moving average for water warmer than 26.5 °C (green), 27.5 °C (blue), and 28.5 °C (purple) in HadGEM3-GC31-HH, HadGEM3-GC31-HM, ECE and CESM

(Roberts et al. 2020b), when compared to lower resolution ocean models. An oceanic decrease in heat transfer to higher latitudes allows heat to accumulate in the tropical Atlantic, and the AWP consequently expands northward and eastward.

To confirm and develop these findings, Lagrangian trajectory analysis of warm water flow into the tropical North Atlantic is undertaken. TRACMASS calculations using output from the HadGEM3-GC31-HH forced run are obtained as 6-month backwards trajectories from particles seeded at 20 °N, on June 30 of each of 10 years in 3 decades: 1951–1960, 2001–2010, and 2041–2050. This latitude is in the middle of the region of warm water analysed in previous sections. The choice of start date, near the beginning of the hurricane season, is motivated by the fact that the observed interannual variability at June 30 is higher than in September (Harris et al. 2023), during which time much of water at this latitude is warmer than 26. 5 °C in most historical years. The variability is significantly correlated with annual major Atlantic basin hurricane counts over 1980–2022, with Pearson Correlation Coefficient of .44, significant at the 95% level (Fig. 4.8).

The mean January—June temperature of warm water (warmer than 26.5 °C) particle tracks ending at 20 °N at the end of June in the HadGEM3-GC31-HH forced run is plotted in Fig. 4.9 (right) for the 3 decades representing pre-industrial

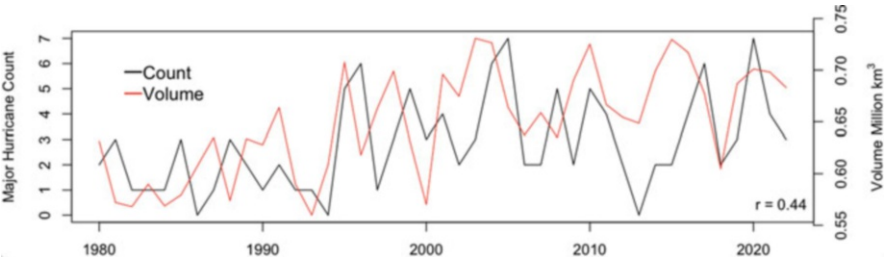

Fig. 4.8 GODAS July 1 volume (million km^3) of water warmer than 26.5 °C between 10 °N and 30 °N (red) and annual major hurricane count (black) 1980–2022

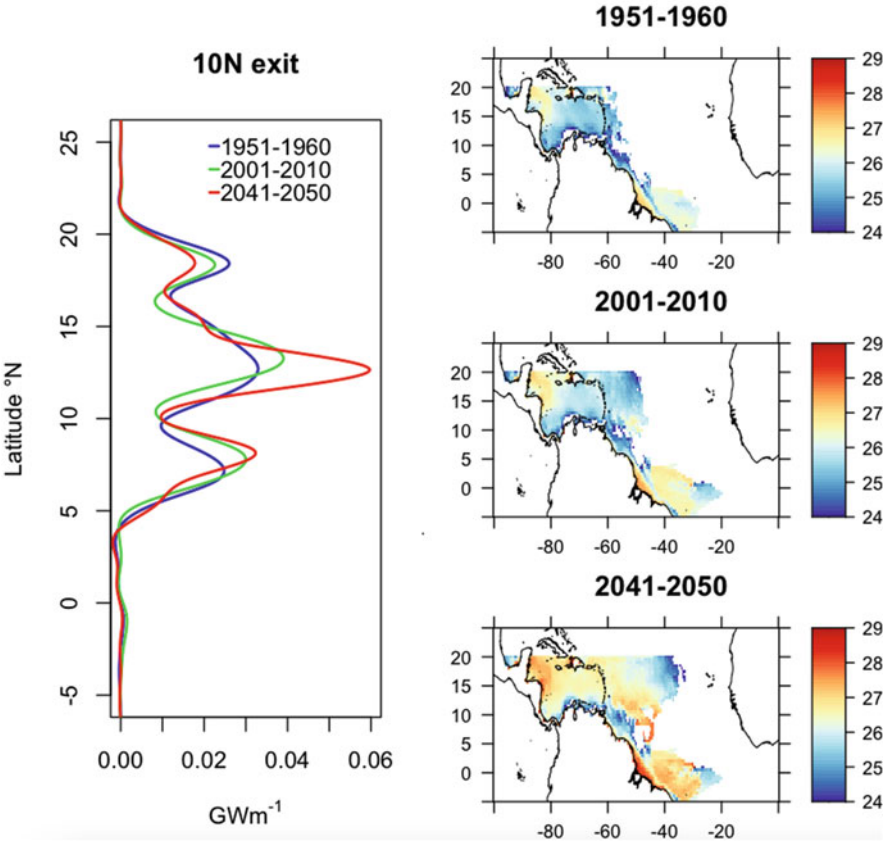

Fig. 4.9 Left: Smoothed mean zonally integrated January–June heat flux into particles back-tracked from 20 °N, which cross 10 °N (GWm^{-1} positive for heat gain) by latitude, averaged over 1951–1960 (blue), 2001–2010 (green), and 2041–2050 (red). Right: January–June mean particle temperature (°C) within 0.5 degree grid boxes averaged over a decade; 1951–1960 (top), 2001–2010 (middle), and 2041–2050 (bottom)

conditions at the start of the model run, 1951–1960 (top), 2001–2010, near the end of the historical forcing (middle), and the last decade of the high emissions forcing, 2041–2050 (bottom). Particle temperatures at all time stamps through the experiment of particles which are located within 0.5 degree grid boxes are averaged, and then averaged over 10 years to smooth interannual variability. The mean temperature of warm water arriving at 20 °N by July 1 is notably warmer near the coast of central America and in the Amazon outflow region in the 2000s than the 1950s. Warm water sources extend 20 degrees further east of the Caribbean. By the 2040s, warm water sources are 2 °C degrees warmer over most of the Caribbean Sea, and 3 °C warmer near the coast of central America and in the Amazon outflow region. Warm water sources extend as far east as 30 °W in the North Atlantic.

The zonally integrated heat flux for particle tracks ending at 20 °N after 6 months, which cross 10 °N, summarises total energy into warm water sources from other regions. This is plotted by latitude in Fig. 4.9 (left). Across all latitudes, the total heat flux along these particle tracks changes very little from the first historical decade (1951–1960, 3.8 GW) to the later historical decade (2001–2010, 3.7 GW). By the final future forced decade (2041–2050), the total heat accumulation along particle tracks crossing 10 °N and ending at 20 °N after 6 months, which are warmer than 26.5 °C, is 14% higher than final historical forced decade (4.2 GW).

Heat flux along these tracks peaks between 12 °N and 14 °N. There is 0.01 GWm^{-1} more zonally-integrated heat convergence at the latitude of smoothed peak heat flux by the present-day decade than the pre-industrial decade, and an additional 0.02 GWm^{-1} of smoothed peak heat flux by the near-future decade than the present-day. In summary, HadGEM3-GC31-HH predicts that more heat will move through the tropical Atlantic from south of 10 °N over the next few decades, with the peak heat flux convergence just north of 10 °N.

This accumulation of heat in the tropical Atlantic is evident in the mean sea temperature map of the 2040s (Fig. 4.9, bottom right), where much warmer water, with temperatures greater than 27 °C, reach 20 °N in the previous 6 months than in the earlier decades, the 1950s and 2000s, where there is less change in the temperature of water parcels approaching 20 °N by July 1.

In summary, two techniques are used here to quantify changes in ocean currents leading to future accumulation of heat in HadGEM3-GC31-HH over the region of recent hurricane development. Advective heat convergence between 10 °N and 30 °N is quantified and compared with other high-resolution models. A complementary technique, Lagrangian heat convergence analysis backwards from 20 °N, is used to confirm findings. Both methods highlight the role of reduced meridional ocean transport in the next few decades, allowing more heat accumulation into the tropical Atlantic by the middle of the century, beginning around the present-day.

4.4 Conclusions

We have quantified changes in the volume of warm water related to increasing ocean heat content, which could be available for hurricane intensification in the tropical North Atlantic in the forced run of a high-resolution ocean model. The pool of warm water becomes more widespread to the north and east, as well as deepening. Quantification of changes in tropical North Atlantic mechanisms, leading to heat accumulation in a high-resolution forced ocean model, provide insight into one factor which could impact future hurricane risk, due an increase in deeper, more extensive pool of warm water which would be available for development of major hurricanes when atmospheric conditions are conducive to tropical deep convection.

This warm water volume is shown here to be positively correlated with annual major Atlantic hurricane counts in the observational record, though climate models suggest lower hurricane frequency in a warmer climate. The HadGEM3-GC31-HH volume of water warmer increases steadily towards 2050, at a higher rate than has been observed, albeit from a lower starting point in the model. This indicates that more intense hurricanes are possible in a warmer climate when atmospheric conditions allow.

While net heat flux into the tropical Atlantic does not increase in the HadGEM3-GC31-HH forced run, the amount of water transformed across warm isotherms does increase, due to the larger surface area of warm water just below these temperatures. However, this increase in the area is itself not expanding because of heat transfer mechanisms from the atmosphere, but due to oceanic processes.

Heat accumulation in this expanding region of warm water in the North Atlantic stems from slower ocean circulation in HadGEM3-GC31-HH. This is quantified by the increasing volume of heat convergence between 10 °N and 30 °N, which is also found in in 3 other high-resolution climate models. Likewise, Lagrangian heat convergence analysis for water arriving at 20 °N by July 1 shows a dramatic increase in warm water parcels by the 2040s, relative to the difference between the changes from the 1950s to the present day. HadGEM3-GC31-HH has the highest climate model ocean resolution available and the largest increase in warm water between latitudes currently relevant to major hurricane development, suggesting that, from an ocean heat perspective, there will be more potential for future hurricane intensification not found in previous climate model studies using lower resolution models.

Ocean heat content is projected to increase due a larger volume of warm water in the tropical Atlantic, driven by slower ocean circulation, if greenhouse gas emissions continue at the present rate. Future climate model runs at even higher resolutions could better resolve oceanic and atmospheric pathways for heat transfer into the tropical Atlantic, as well as detecting intense hurricanes themselves, and overcoming SST biases, which would increase confidence in future hurricane activity projections.

Acknowledgements The ORCA12 hindcast was led by Dr. Alex Megann of the National Oceanography Centre. The HighResMIP simulations were undertaken by many dedicated colleagues, who have kindly provided the community with access to the model data. Analysis of the ORCA12 hindcast and HighResMIP simulations was undertaken on JASMIN, the UK collaborative data analysis facility. We acknowledge Dr. Jeffrey Blundell from the University of Southampton, UK for his unconditional support in setting up TRACMASS on JASMIN.

References

Aiyyer AR, Thorncroft C (2006) Climatology of vertical wind shear over the tropical Atlantic. J Clim 19(12):2969–2983

Aldama-Campino A, Döös K, Kjellsson J, Jönsson B (2020) TRACMASS: formal release of version 7.0 (version v7.0-beta). Zenodo. https://doi.org/10.5281/zenodo.4337926

Behringer D, Xue Y (2004, January) Evaluation of the global ocean data assimilation system at NCEP: the Pacific Ocean. In Eighth Symp. on Integrated Observing and Assimilation Systems for Atmosphere, Oceans, and Land Surface

Bellomo K, Angeloni M, Corti S, von Hardenberg J (2021) Future climate change shaped by inter-model differences in Atlantic meridional overturning circulation response. Nat Commun 12(1): 3659

Chan D, Vecchi GA, Yang W, Huybers P (2021) Improved simulation of 19th-and 20th-century North Atlantic hurricane frequency after correcting historical sea surface temperatures. Sci Adv 7(26):eabg6931

Danabasoglu G (2008) On multidecadal variability of the Atlantic meridional overturning circulation in the community climate system model version 3. J Clim 21(21):5524–5544

Danabasoglu G, Bates SC, Briegleb BP, Jayne SR, Jochum M, Large WG, ... Yeager SG (2012) The CCSM4 ocean component. J Clim 25(5):1361–1389

Dare RA, McBride JL (2011) The threshold sea surface temperature condition for tropical cyclogenesis. J Clim 24(17):4570–4576

Davis CA (2018) Resolving tropical cyclone intensity in models. Geophys Res Lett 45:2082–2087

DeMaria M, Knaff JA, Connell BH (2001) A tropical cyclone genesis parameter for the tropical Atlantic. Weather Forecast 16(2):219–233

Domingues R, Kuwano-Yoshida A, Chardon-Maldonado P, Todd RE, Halliwell G, Kim HS et al (2019) Ocean observations in support of studies and forecasts of tropical and extratropical cyclones. Front Mar Sci 6:446

Döös K, Jönsson B, Kjellsson J (2017) Evaluation of oceanic and atmospheric trajectory schemes in the TRACMASS trajectory model v6. 0. Geosci Model Dev 10(4):1733–1749

Dunstone NJ, Smith DM, Booth BBB, Hermanson L, Eade R (2013) Anthropogenic aerosol forcing of Atlantic tropical storms. Nat Geosci 6(7):534–539

Emanuel K (2021) Response of global tropical cyclone activity to increasing CO_2: results from downscaling CMIP6 models. J Clim 34(1):57–70

Evans JL, Waters JJ (2012) Simulated relationships between sea surface temperatures and tropical convection in climate models and their implications for tropical cyclone activity. J Clim 25(22): 7884–7895

Goldenberg SB, Landsea CW, Mestas-Nuñez AM, Gray WM (2001) The recent increase in Atlantic hurricane activity: causes and implications. Science 293(5529):474–479

Good SA, Martin MJ, Rayner NA (2013) EN4: quality controlled ocean temperature and salinity profiles and monthly objective analyses with uncertainty estimates. J Geophys Res Oceans 118(12):6704–6716

Groeskamp S, Griffies SM, Iudicone D, Marsh R, Nurser AG, Zika JD (2019) The water mass transformation framework for ocean physics and biogeochemistry. Annu Rev Mar Sci 11(1): 271–305

Haarsma RJ, Roberts MJ, Vidale PL, Senior CA, Bellucci A, Bao Q et al (2016) High resolution model intercomparison project (HighResMIP v1. 0) for CMIP6. Geosci Model Dev 9(11): 4185–4208

Haarsma R, Acosta Cobos MC, Bakhshi R, Bretonnière PA, Caron LP, Castrillo M et al (2020) HighResMIP versions of EC-earth: EC-Earth3P and EC-Earth3P-HR–description, model computational performance and basic validation. Geosci Model Dev 13(8):3507–3527

Hall T, Hereid K (2015) The frequency and duration of US hurricane droughts. Geophys Res Lett 42(9):3482–3485

Hallam S, Marsh R, Josey SA, Hyder P, Moat B, Hirschi JJM (2019) Ocean precursors to the extreme Atlantic 2017 hurricane season. Nat Commun 10(1):1–10
Hallam S, Guishard M, Josey SA, Hyder P, Hirschi J (2021) Increasing tropical cyclone intensity and potential intensity in the subtropical Atlantic around Bermuda from an ocean heat content perspective 1955–2019. Environ Res Lett 16(3):034052
Han Y, Zhang MZ, Xu Z, Guo W (2021) Assessing the performance of 33 CMIP6 models in simulating the large-scale environmental fields of tropical cyclones. Clim Dyn:1–16
Harris E, Marsh R, Grist JP, McCarthy GD (2022) The water mass transformation framework and variability in hurricane activity. Clim Dyn 59(3–4):961–972
Harris EA, Marsh R, Grist JP (2023) Tracing oceanic sources of heat content available for Atlantic hurricanes. J Geophys Res Oceans 128, e2022JC019407(5)
Hersbach H, Bell B, Berrisford P, Hirahara S, Horányi A, Muñoz-Sabater J et al (2020) The ERA5 global reanalysis. Q J R Meteorol Soc 146(730):1999–2049
Johnson NC, Xie SP (2010) Changes in the sea surface temperature threshold for tropical convection. Nat Geosci 3(12):842–845
Kang NY, Elsner JB (2015) Trade-off between intensity and frequency of global tropical cyclones. Nat Clim Chang 5(7):661–664
Klotzbach PJ, Bowen SG, Pielke R, Bell M (2018) Continental US hurricane landfall frequency and associated damage: observations and future risks. Bull Am Meteorol Soc 99(7):1359–1376
Knapp KR, Kruk MC, Levinson DH, Diamond HJ, Neumann CJ (2010) The international best track archive for climate stewardship (IBTrACS) unifying tropical cyclone data. Bull Am Meteorol Soc 91(3):363–376
Knapp KR, Diamond HJ, Kossin JP, Kruk MC, Schreck CJ (2018) International best track archive for climate stewardship (IBTrACS) project, version 4. NOAA National Centers for Environmental Information
Knutson T, Camargo SJ, Chan JC, Emanuel K, Ho CH, Kossin J et al (2019) Tropical cyclones and climate change assessment: part I: detection and attribution. Bull Am Meteorol Soc 100(10): 1987–2007
Knutson T, Camargo SJ, Chan JC, Emanuel K, Ho CH, Kossin J et al (2020) Tropical cyclones and climate change assessment: part II: projected response to anthropogenic warming. Bull Am Meteorol Soc 101(3):E303–E322
Korty RL, Camargo SJ, Galewsky J (2012) Tropical cyclone genesis factors in simulations of the last glacial maximum. J Clim 25(12):4348–4365
Lin II, Camargo SJ, Patricola CM, Boucharel J, Chand S, Klotzbach P, . . . Jin FF (2020) ENSO and tropical cyclones. El Niño Southern Oscillation in a changing climate, 377–408
Liu H, Wang C, Lee SK, Enfield D (2013) Atlantic warm pool variability in the CMIP5 simulations. J Clim 26(15):5315–5336
Madan G, Gjermundsen A, Iversen SC, LaCasce JH (2023) The weakening AMOC under extreme climate change. Clim Dyn 62(2):1–19
Madec G, Bourdallé-Badie R, Bouttier PA, Bricaud C, Bruciaferri D, Calvert D, Vancoppenolle M (2017) NEMO ocean engine (Version v3. 6), Notes du Pôle de modélisation de l'Institut Pierre-simon Laplace (IPSL), 27, Zenodo
Mayer J, Haimberger L, Mayer M (2023) A quantitative assessment of air-sea heat flux trends from ERA5 since 1950 in the North Atlantic basin. Earth Syst Dyn Discuss 2023:1–36
McTaggart-Cowan R, Davies EL, Fairman JG, Galarneau TJ, Schultz DM (2015) Revisiting the 26.5° C Sea surface temperature threshold for tropical cyclone development. Bull Am Meteorol Soc 96(11):1929–1943
Moharana SS, Swain D (2023) On the recent increase in Atlantic Ocean hurricane activity and influencing factors. Nat Hazards 118(2):1–13
Murakami H, Levin E, Delworth TL, Gudgel R, Hsu PC (2018) Dominant effect of relative tropical Atlantic warming on major hurricane occurrence. Science 362(6416):794–799
NOAA National Centers for Environmental Information (NCEI) (2023) US billion-dollar weather and climate disasters. https://doi.org/10.25921/stkw-7w73

Nyberg J, Malmgren BA, Winter A, Jury MR, Kilbourne KH, Quinn TM (2007) Low Atlantic hurricane activity in the 1970s and 1980s compared to the past 270 years. Nature 447(7145): 698–701

Pfleiderer P, Nath S, Schleussner CF (2022) Extreme Atlantic hurricane seasons made twice as likely by ocean warming. Weather Clim Dyn 3(2):471–482

Roberts MJ, Baker A, Blockley EW, Calvert D, Coward A, Hewitt HT et al (2019) Description of the resolution hierarchy of the global coupled HadGEM3-GC3. 1 model as used in CMIP6 HighResMIP experiments. Geosci Model Dev 12(12):4999–5028

Roberts MJ, Camp J, Seddon J, Vidale PL, Hodges K, Vannière B et al (2020a) Projected future changes in tropical cyclones using the CMIP6 HighResMIP multimodel ensemble. Geophys Res Lett 47(14):e2020GL088662

Roberts MJ, Jackson LC, Roberts CD, Meccia V, Docquier D, Koenigk T et al (2020b) Sensitivity of the Atlantic meridional overturning circulation to model resolution in CMIP6 HighResMIP simulations and implications for future changes. JAMES 12(8):e2019MS002014

Rousseau-Rizzi R, Emanuel K (2022) Natural and anthropogenic contributions to the hurricane drought of the 1970s–1980s. Nat Commun 13(1):5074

Saunders MA, Lea AS (2008) Large contribution of sea surface warming to recent increase in Atlantic hurricane activity. Nature 451(7178):557–560

Small RJ, Bacmeister J, Bailey D, Baker A, Bishop S, Bryan F et al (2014) A new synoptic scale resolving global climate simulation using the community earth system model. J Adv Model Earth Syst 6(4):1065–1094

Sobel AH, Wing AA, Camargo SJ, Patricola CM, Vecchi GA, Lee CY, Tippett MK (2021) Tropical cyclone frequency. Earth's Future 9(12):e2021EF002275

Sugi M, Yoshida K, Murakami H (2015) More tropical cyclones in a cooler climate. Geophys Res Lett 42(16):6780–6784

Tang B, Camargo SJ (2014) Environmental control of tropical cyclones in CMIP5: a ventilation perspective. J Adv Model Earth Syst 6(1):115–128

Vecchi GA, Soden BJ (2007) Increased tropical Atlantic wind shear in model projections of global warming. Geophys Res Lett 34(8)

Vecchi GA, Landsea C, Zhang W, Villarini G, Knutson T (2021) Changes in Atlantic major hurricane frequency since the late-19th century. Nat Commun 12(1):4054

Walin G (1982) On the relation between sea-surface heat flow and thermal circulation in the ocean. Tellus 34(2):187–195

Walsh KJ, McBride JL, Klotzbach PJ, Balachandran S, Camargo SJ, Holland G, ... Sugi M (2016) Tropical cyclones and climate change. Wiley Interdiscip Rev Clim Chang 7(1):65–89

Wang C, Lee SK (2007) Atlantic warm pool, Caribbean low-level jet, and their potential impact on Atlantic hurricanes. Geophys Res Lett 34(2):L02703

Wang C, Liu H, Lee SK, Atlas R (2011) Impact of the Atlantic warm pool on United States landfalling hurricanes. Geophys Res Lett 38(19):L19702

Weaver MM, Garner AJ (2023) Varying genesis and landfall locations for North Atlantic tropical cyclones in a warmer climate. Sci Rep 13(1):5482

Yan X, Zhang R, Knutson TR (2017) The role of Atlantic overturning circulation in the recent decline of Atlantic major hurricane frequency. Nat Commun 8(1):1–8

Yoshida K, Sugi M, Mizuta R, Murakami H, Ishii M (2017) Future changes in tropical cyclone activity in high-resolution large-ensemble simulations. Geophys Res Lett 44(19):9910–9917

Zhang R, Sutton R, Danabasoglu G, Kwon Y-O, Marsh R, Yeager SG, Amrhein DE, Little CM (2019) A review of the role of the Atlantic meridional overturning circulation in Atlantic multidecadal variability and associated climate impacts. Rev Geophys 57(2):316–375